A method for measuring methane oxidation rates using low-levels of ^{14}C-labeled methane and accelerator mass spectrometry

Mary A. Pack[1]*, Monica B. Heintz[2], William S. Reeburgh[1], Susan E. Trumbore[1], David L. Valentine[2], Xiaomei Xu[1], and Ellen R. M. Druffel[1]

[1]University of California Irvine, Irvine, California 92697
[2]University of California Santa Barbara, Santa Barbara, California 93106
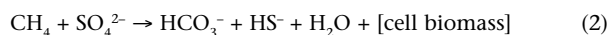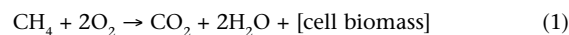
Abstract

We report a new method for methane oxidation rate measurements that uses 10^3-10^5 times less ^{14}C-CH$_4$ than existing measurements by taking advantage of the high sensitivity of accelerator mass spectrometry. Methane oxidation in the marine environment is a microbial process of global importance because it prevents methane released from underlying reservoirs from reaching the ocean and atmosphere. Rate measurements provide a crucial tool for assessing the efficacy of this process across a range of environments, but the current methods use high amounts of radioactive elements (^{3}H- or ^{14}C-CH$_4$), tend to increase methane concentrations in a sample markedly over in situ levels, and are limited by strict health and safety regulations. The low-level method presented here uses levels of ^{14}C-CH$_4$ that are below transportation regulations, produce samples that do not require treatment as radioactive waste, and allow for tracer level rate measurements in low methane environments. Moreover, the low-level method lays the analytical foundation for a below-regulation rate measurement that could be used broadly and in-situ. Parallel rate measurements with the low-level ^{14}C-CH$_4$ and existing ^{3}H-CH$_4$ methods are generally consistent with a correlation coefficient of 0.77. However, the low-level method in most cases yields slower rates than the ^{3}H method possibly due to temperature, priming, and detection limit effects.

Marine methane oxidation consumes 80% (85-304 Tg CH$_4$ y^{-1}; Hinrichs and Boetius 2002; Reeburgh 2007) or more of the methane (CH$_4$) released from sediments and is a globally important sink for the potent greenhouse gas. Measurements of marine methane oxidation rates, however, are sparse and the environmental controls on oxidation are not well understood. Further, scaling the available rate measurements to the world ocean introduces large uncertainties to estimates of total marine methane consumption (the range is large: 85-304 Tg CH$_4$ yr^{-1}).

Methane oxidation occurs by two distinct processes in oxic and anoxic environments. Aerobic methane oxidation (Eq. 1) is mediated by methanotrophs (bacteria capable of using CH$_4$ as their sole source of carbon and energy), whereas anaerobic oxidation of methane (AOM; Eq. 2) is mediated by archea in consortia with sulfate reducing bacteria (Reeburgh 2007). Recent studies show that AOM in low sulfate environments may be coupled with nitrate, iron, or manganese instead of sulfate (e.g., Beal et al. 2009; Caldwell et al. 2008; Crowe et al. 2010; Raghoebarsing et al. 2006). For either process, after methane is fixed, its carbon can be respired for energy or incorporated into the microbe's cell biomass.

$$CH_4 + 2O_2 \rightarrow CO_2 + 2H_2O + \text{[cell biomass]} \tag{1}$$

$$CH_4 + SO_4^{2-} \rightarrow HCO_3^- + HS^- + H_2O + \text{[cell biomass]} \tag{2}$$

Rates of the above reactions in water columns and sediments have been measured by radiotracer (^{14}C-CH$_4$ or ^{3}H-CH$_4$) methods (e.g., Alperin and Reeburgh 1985; Carini et al. 2005; Griffiths et al. 1982; Hoehler et al. 1994; Joye et al. 2004; Joye et al. 1999; Reeburgh et al. 1991; Reeburgh 1980; Treude et al. 2003; Valentine et al. 2010; Valentine et al. 2001), stable isotope tracer (^{13}C-CH$_4$) methods (e.g., Moran et al. 2008; Moran et al. 2007), tracking changes in methane concentration over time in discrete samples (e.g., Carini et al. 2003; Girguis et al.

2005; Girguis et al. 2003; Nauhaus et al. 2002; Sansone and Martens 1978), comparing water mass age with methane saturation and modeling methane turnover (water column only; e.g., Heeschen et al. 2004; Rehder et al. 1999; Scranton and Brewer 1978), and one-dimensional numerical models with sediment CH_4 and sulfate profiles (sediment AOM only; e.g., Jørgensen et al. 2001). Radiotracer methods measure the incorporation of $^3H\text{-}CH_4$ or $^{14}C\text{-}CH_4$ tracers in the oxidation products during a timed incubation by decay-counting. These methods are the most sensitive and direct of the available methods and are thus the most commonly used (Heintz 2011). Stable isotope tracer ($^{13}C\text{-}CH_4$) methods are not viable in the marine environment due to the large amount of ^{13}C in the dissolved inorganic carbon (DIC: carbon dioxide, carbonic acid, and carbonate and bicarbonate ions) pool. The amount of carbon dioxide (CO_2) typically produced by methane oxidation during short incubations (1 d) is too small compared with natural $^{13}C\text{-}DIC$ to create a signal that is detectable by mass spectrometry.

Rate measurements of marine methane oxidation are sparse because the commonly used radiotracer methods (RT methods) are logistically complex. Difficulties with international shipping of radioisotopes, concerns for possible contamination of sensitive natural abundance measurements (^{14}C and ^3H), strict health and safety regulations for handling radioisotopes in lab and nonlab settings (Table 1), and high costs associated with radioactive material training, regulation, and waste disposal all limit the usefulness of the RT rate measurements. In addition, regulations and permitting for radioactive applications are especially difficult in Arctic environments (an area of special interest in methane cycling) and rapid response situations (e.g., the Gulf of Mexico oil spill) and have become stricter overall in recent years (Rudd et al. 1974 versus King et al. 2002).

Here we introduce a $^{14}C\text{-}CH_4$ RT method that uses $10^3\text{-}10^5$ less ^{14}C than existing RT methods by replacing decay-counting with accelerator mass spectrometry (AMS). AMS detects individual atoms rather than decay events and can make $10^3\text{-}10^9$ more sensitive ^{14}C measurements (Turteltaub and Vogel 2000). The low-level radiotracer method (LLRT method) adds 0.0146 kBq $^{14}C\text{-}CH_4$ per sample compared with the 370 kBq $^3H\text{-}CH_4$ added by an existing RT method (Table 2), yet still raises the background $^{14}C\text{-}CH_4$ by a factor of 10^7. Incubating a water sample (120 mL, 100 nM CH_4, 0.6 nM CH_4 d^{-1} oxidation rate) with the low-level $^{14}C\text{-}CH_4$ for 1 d will raise the ^{14}C-concentration in the oxidation products by a factor of 120-140. This increase in ^{14}C is below the minimum detection limit for standard decay-counting techniques, but is easily detected by AMS. The LLRT method uses levels of $^{14}C\text{-}CH_4$ that are considered exempt for transportation regulations and lays the analytical foundation for a rate measurement that is below regulated levels (Table 1). In addition, the method produces labeled samples that do not require treatment as radioactive waste (Table 1) and allows for tracer level measurements in low CH_4 environments because it uses $30\text{-}10^3$ times less CH_4 per sample than existing RT methods (Table 2). Thus, the LLRT method introduced here and below-regulation RT methods to follow will be useful for routine methane oxidation rate measurements in low-methane environments and when application of the existing RT methods for oxidation rate measurements is not practical.

Table 1. United States Code of Federal Regulations (CFR) concerning the use of ^{14}C-labeled radioactive material for academic research as of 2010. These regulations apply in U.S. ocean waters. For research carried out at land-based field sites within the U.S., one will need to look-up and follow regulations put forth by the state in which the field site is located.

Activity	Regulating law	Exempt quantities for ^{14}C	
		Concentration	Total
Use/possession	CFR Title 10. Chapter 1.* *(licensing)*	0.037 Bq/mL (gas)	3.7×10^6 Bq
		296 Bq/mL (liquid)	
Transportation	CFR Title 49. Subtitle B. Chapter 1. Volume 2. Subchapter C.	10^4 Bq/g	10^7 Bq
Waste disposal	CFR Title 10. Chapter 1. Volume 1. Part 20. Subpart K. §2005.	1850 Bq/g	—

Below-regulation = below all regulations listed here.
*Exempt here = below both the total activity and concentration activity.

Table 2. Summary of the radioactive tracers used for water column methane oxidation rate measurements and their characteristics.

Tracer	Products	Quantification	Tracer activity		Added to sample	Methane increase
			Bq/g	Bq/mL	kBq	nM*
$^{14}C\text{-}CH_4$	$^{14}C\text{-}CO_2$, $^{14}C\text{-}Cell$	decay counting	$1.1\text{-}3.9 \times 10^{10}$	$1.3\text{-}4.4 \times 10^6$	93-880	1800-2700
$^3H\text{-}CH_4$	$[^3H\text{-}H_2O, {}^3H\text{-}Cell]$	decay counting	$3.7\text{-}6.4 \times 10^9$	$3.5\text{-}7.4 \times 10^6$	350-370	12.5-25
Low-level $^{14}C\text{-}CH_4$	$^{14}C\text{-}CO_2$, $^{14}C\text{-}Cell$	AMS	1.6×10^5	292	0.0146	0.41

Data from Valentine et al. (2001), Ward (1992), Ward et al. (1989), and David Valentine's Lab at UC Santa Barbara.
*Methane increase following injection of tracer into a 160-mL water sample for the existing ^{14}C- and $^3H\text{-}CH_4$ tracers and 120 mL for the low-level $^{14}C\text{-}CH_4$ tracer.

Materials and procedures

As outlined in Fig. 1, the ^{14}C-CH_4 LLRT method has 6 steps: [1] collecting fresh water samples, [2] treating the samples with low-levels of ^{14}C-CH_4 and incubating, [3] killing and removing the unreacted CH_4, [4] measuring the increase in the ^{14}C-DIC by AMS, [5] measuring the increase in the ^{14}C-cell biomass by AMS, and [6] calculating oxidation rates. Steps 1-3 are carried out shipboard, while steps 4-6 are completed in a land-based laboratory. A detailed description of each step and information on preparation and activity measurements of the low-level ^{14}C-CH_4 tracer are provided below.

To measure the increase in the ^{14}C-DIC and ^{14}C-cell biomass that occurs during incubation with ^{14}C-CH_4 tracer, two sample types are needed: one labeled and one natural/background. Labeled samples are inoculated with ^{14}C-CH_4 (ca. 1 µmol L^{-1} CH_4 in ^{14}C-free CO_2) and treated as outlined below, whereas natural samples are subject to the same process but only treated with ^{14}C-free CO_2. When developing the LLRT method, we focused on the oxic/suboxic water column where methane oxidation is expected to follow the aerobic pathway outlined in Eq. 1. The products of aerobic oxidation are water, CO_2, and

cell biomass. After CO_2 is formed, it mixes with the ambient DIC pool, thus our measurements deal with DIC, not dissolved CO_2.

Preparation of the ^{14}C-CH_4 tracer

The low-level ^{14}C-CH_4 tracer used here originated from parent ^{14}C-CH_4 that was prepared according to methods outlined in Daniels and Zeikus (1983). The parent ^{14}C-CH_4 was 16 mmol L^{-1} CH_4 in hydrogen and contained 3.4×10^6 Bq ^{14}C mL^{-1}. Our ^{14}C-CH_4 tracer was prepared by diluting a ~1 mL aliquot of the parent ^{14}C-CH_4 in 16 L of ^{14}C-free CO_2 in a pre-evacuated 6 L stainless steel gas canister. We chose CO_2 as the carrier gas for our ^{14}C-CH_4 tracer because of its high solubility in sea water, but other reasonably soluble carrier gasses such as nitrogen may also be used. The low-level ^{14}C-CH_4 tracer had a final activity concentration of 292 Bq mL^{-1} (1.6×10^5 Bq g^{-1}), with a total of 4.8×10^6 Bq and 1.7 atmg pressure in the gas canister. For details on tracer activity measurements, refer to the "*Activity of the ^{14}C-CH_4 tracer*" section.

Note that we prepared our ^{14}C-CH_4 tracer with a higher activity concentration (more ^{14}C delivered per sample) than necessary so that the efficacy of the LLRT method could be tested with ease. The higher activity added a step to the ^{14}C-
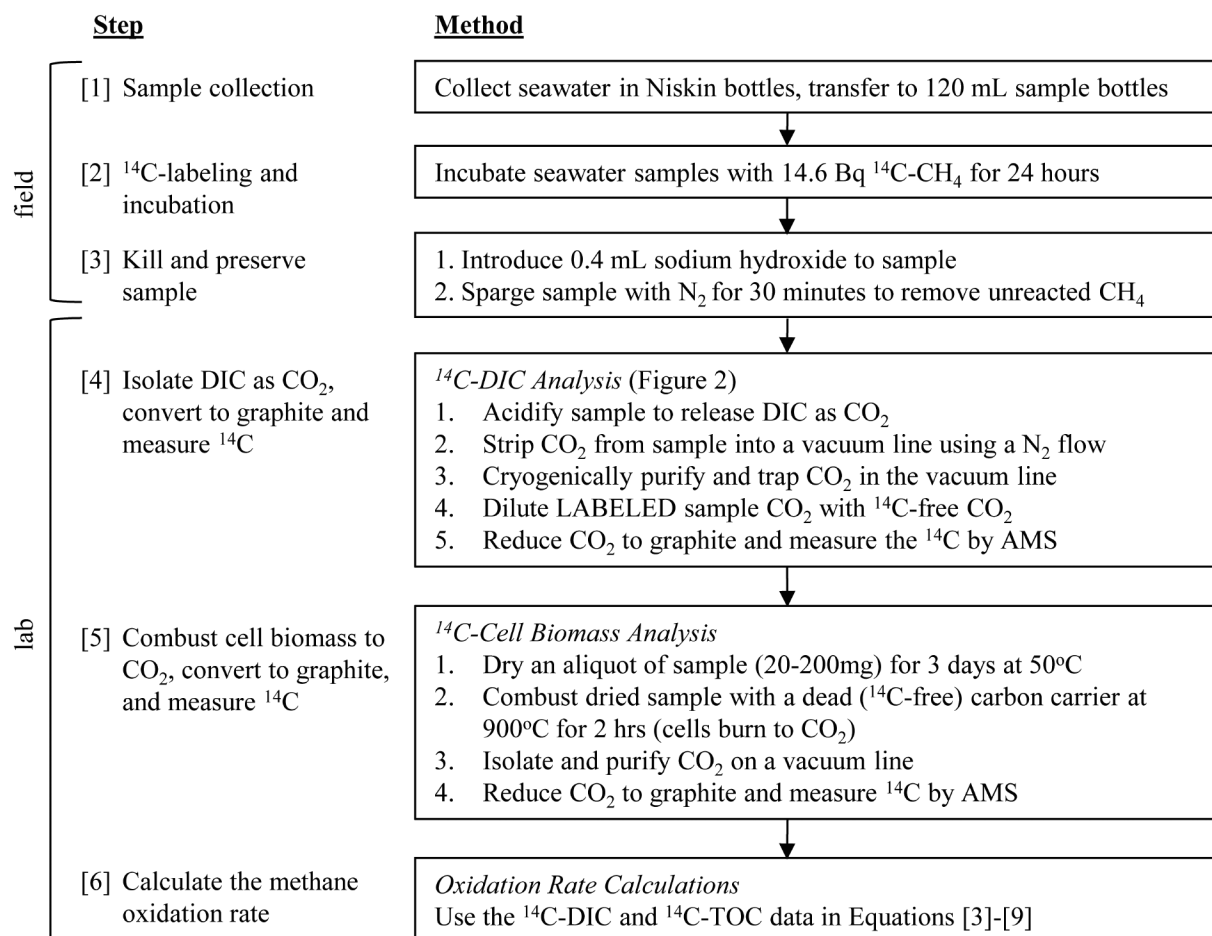
Step	Method
[1] Sample collection	Collect seawater in Niskin bottles, transfer to 120 mL sample bottles
[2] ^{14}C-labeling and incubation	Incubate seawater samples with 14.6 Bq ^{14}C-CH_4 for 24 hours
[3] Kill and preserve sample	1. Introduce 0.4 mL sodium hydroxide to sample 2. Sparge sample with N_2 for 30 minutes to remove unreacted CH_4
[4] Isolate DIC as CO_2, convert to graphite and measure ^{14}C	*^{14}C-DIC Analysis* (Figure 2) 1. Acidify sample to release DIC as CO_2 2. Strip CO_2 from sample into a vacuum line using a N_2 flow 3. Cryogenically purify and trap CO_2 in the vacuum line 4. Dilute LABELED sample CO_2 with ^{14}C-free CO_2 5. Reduce CO_2 to graphite and measure the ^{14}C by AMS
[5] Combust cell biomass to CO_2, convert to graphite, and measure ^{14}C	*^{14}C-Cell Biomass Analysis* 1. Dry an aliquot of sample (20-200mg) for 3 days at 50°C 2. Combust dried sample with a dead (^{14}C-free) carbon carrier at 900°C for 2 hrs (cells burn to CO_2) 3. Isolate and purify CO_2 on a vacuum line 4. Reduce CO_2 to graphite and measure ^{14}C by AMS
[6] Calculate the methane oxidation rate	*Oxidation Rate Calculations* Use the ^{14}C-DIC and ^{14}C-TOC data in Equations [3]-[9]

Steps [1]-[3] are grouped as *field*; steps [4]-[6] are grouped as *lab*.

Fig. 1. Summary of the ^{14}C-CH_4 LLRT rate measurement procedures.

DIC analysis with the labeled samples; their ^{14}C-content was above the maximum AMS detection limit (ca. 8 times modern under the standard operating conditions at the UC Irvine Keck Carbon Cycle AMS facility) and they required dilution before analysis. This extra step can removed from the analysis procedure if the ^{14}C-CH_4 tracer is prepared with an activity level appropriate for the environment in which it will be applied. Such considerations are discussed in the "*Comments and recommendations*" section.

Step 1: Sample collection

Water samples were collected in 10 L Niskin bottles attached to a conductivity-temperature-depth (CTD)/Rosette. Four 120 mL glass serum bottles (Wheaton Scientific #223747; pre-weighed and washed three times with 5% hydrochloric acid and deionized water and dried at 110°C) were filled directly from each Niskin bottle using Tygon tubing secured to a 6-inch length of Pyrex tubing. Bottles were rinsed three times with sample before they were filled from the bottom to overflowing. The sample bottles were then sealed without air bubbles with gray butyl stoppers and aluminum crimp caps (Wheaton Scientific #W224100-193 and 22417-01). The four samples collected were divided into duplicate sets of labeled and natural samples.

Step 2: ^{14}C-labeling and incubation

This section outlines the labeling and incubation procedures used for labeled samples. Natural samples were treated identically, but injected with ^{14}C-free CO_2 instead of ^{14}C-CH_4 tracer using a designated syringe. The ^{14}C-CH_4 tracer was introduced to samples in sets of 10-20 using a gastight Hamilton syringe (100 μL with removable needle and reproducibility adapter, Hamilton Company #81030 and 14725). The Hamilton syringe was purged 3 times with ^{14}C-CH_4 before starting tracer additions and 50 μL tracer aliquots (with 14.6 Bq ^{14}C, 6.3×10^{-12} mol ^{14}C) were prepared for each sample by filling the Hamilton syringe to 80 μL and venting to 50 μL using the stop bottom on the reproducibility adapter. The ^{14}C-CH_4 tracer aliquots were introduced to samples using a two syringe technique: the sample stopper was pierced with the needle of a vent syringe to receive displaced water, the Hamilton syringe needle was inserted in the stopper, the tracer aliquot was introduced, and the Hamilton syringe needle was removed followed by the vent syringe needle. Last, samples were shaken vigorously for 1 min to equilibrate the ^{14}C-CH_4 with the liquid phase and incubated upside down in the dark for 24 h at near in situ temperatures.

Step 3: Killing and removal of unreacted CH_4

The following post incubation procedures for labeled and natural samples were carried out inside a glove bag (Glass-Col #108DX-37-27H) that was purged and partially inflated with ultra-high purity nitrogen (UHP N_2). The N_2 filled glove bag prevented sample exposure to atmospheric CO_2 that can alter the ^{14}C-DIC, and natural and labeled samples were processed in separate glove bags to prevent cross contamination. First, 0.4 mL sodium hydroxide (NaOH, saturated and bicarbonate free) were added to samples using the two syringe technique described above and samples were vigorously shaken for 30 s. This treatment ended the incubation period by killing samples (stopping microbial activity) and converting the gaseous CO_2 oxidation product to aqueous carbonate. Next, sample stoppers were removed, 60 mL from each sample were poured into a waste container, and samples were sparged for 30 min with UHP N_2 to remove the unreacted CH_4. A basic kill agent (NaOH) has been used in previously published ^{14}C-CH_4 RT studies and is necessary as opposed to a metabolic kill agent (e.g., mercuric chloride) to sequester the CO_2 in solution so that it is not removed with the unreacted CH_4. Finally, samples were resealed with blue butyl rubber stoppers (Bellco Glass #2048-11800) and aluminum crimp caps, removed from the glove bag, and stored upside down for transport back to shore.

Step 4: ^{14}C-DIC analysis

DIC from natural and labeled samples was prepared for ^{14}C-AMS analysis using a continuous flow vacuum line (Fig. 2) similar to Blumhagen and Clark (2008), McNichol et al. (1994), and Pohlman et al. (2000). The procedure involves 5 steps: (A) acidifying the sample to release the DIC as CO_2, (B) stripping the CO_2 from the sample into a vacuum line with a flow of UHP N_2 (i.e., sample sparging), (C) cryogenically purifying and trapping the CO_2 in the vacuum line, (D) quantifying the recovered CO_2, and (E) reducing CO_2 to graphite, dilut-
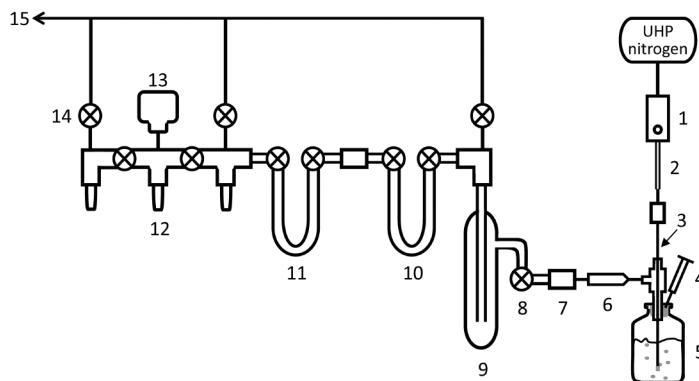

Fig. 2. DIC extraction line: (1) flowmeter (0-500 mL min^{-1}), (2) nitrogen outlet—delivers nitrogen to the sample through polypropylene tubing (1/4-inch OD) terminating with a male luer-lock adapter (Cole-Parmer# R-31507-27) with a 23 g, 1-inch needle, (3) stripping probe (see Fig. 3 for details), (4) acid syringe: 3 mL plastic syringe with 2 mL degassed phosphoric acid, 85%, and 23 g, 1-inch needle, (5) serum bottle (120 mL) with 60 mL of sample, (6) buffer volume: 1 mL syringe barrel cut through its diameter at the top with a septum stopper (Sigma-Aldrich #Z100714) placed in the top and a 23 g, 1-inch needle, (7) Swagelok Ultra-Torr 1/4-inch union fitted with a 23 g, 1-inch needle at the right, (8) sample valve: stem valve separating the sample from the vacuum line, (9) water trap cooled with dry ice-ethanol slush, (10) water trap with glass beads cooled with dry ice-ethanol slush, (11) CO_2 trap with glass beads cooled with LN$_2$, (12) calibrated volume, (13) Baratron (MKS Instruments) digital pressure gauge, (14) vacuum valve: plug valve used to regulate vacuum extent during DIC extraction, (15) vacuum pump, and (⊗) valve.

ing labeled samples, and measuring sample ^{14}C by AMS. The N_2 flow into the sample combined with the maintenance of a vacuum downstream of the sample creates a continuous flow of gas that allows CO_2 to be stripped from the sample and carried into the vacuum line. A description of each step and details for preparation and operation of the vacuum line are given below.

Sample preparation for DIC extraction

Efficient sparging of samples was accomplished using stripping probes (Fig. 3) designed for the 120 mL sample bottles. The probes were inserted in the sample bottles just prior to extraction in a CO_2-free atmosphere by placing a sample and stripping probe (pre-purged with N_2) in a loosely sealed chamber and flushing the chamber with UHP N_2 for 5 min. Inside the chamber with the N_2 gas still flowing, the sample stopper was removed and the stripping probe inserted. Last, the weight of the sample/stripping probe combination was recorded and the needle of a degassed phosphoric acid filled syringe (Fig. 2, #4) was inserted partway in the stripping probe stopper.

Vacuum line preparation for DIC extractions (numbers in parenthesis below refer to numbers in Fig. 2)

At the start of each extraction, the vacuum line was evacuated, dry ice ethanol slushes were added to the water traps (9 and 10), and a homemade union (a 1 mL plastic syringe barrel cut through its diameter to form a 1/2-inch long tube and septum, Sigma-Aldrich #Z100714, inserted into both ends of the tube) was placed between the nitrogen outlet (2) and buffer volume (6) to substitute for a sample (3-5). The entire line (1-14, with the union substituting for 3-5) was flushed with UHP N_2 and evacuated twice before it was filled to ca. 780 torr. Next, the vacuum line (8-14) was isolated and evacuated, and the nitrogen outlet (2) was flushed by removing its needle from the union and turning the flowmeter (1) to maximum flow. Last, once the vacuum line (8-14) was completely evacuated, a Dewar of liquid nitrogen (LN_2) was placed on the CO_2 trap (11), and the sample with stripping probe (3-5) was attached to the vacuum line; the union was removed from the buffer volume (6) and the buffer volume needle was inserted in the stripping probe (3) outlet, and then the flowmeter (1) was turned off and the nitrogen outlet needle (2) placed in the stripping probe (3) inlet.

Sample acidification, sparging, and purification (Steps A-C)

The sample headspace was sequentially expanded to the water trap (10) and then to the vacuum valve (14) waiting ca. 30 s after each expansion for water vapor to freeze down. Next, the line pressure (created by the sample headspace and read at 13) was pumped down to ca. 100 mtorr by partially opening the vacuum valve (14). While the line pressure decreased, the acid syringe (4) needle was pushed through the stripping probe (3) stopper, the degassed phosphoric acid injected, and the needle removed.

As the line pressure approached 100 mtorr, N_2 was introduced to the line (the flowmeter was turned on) and sample
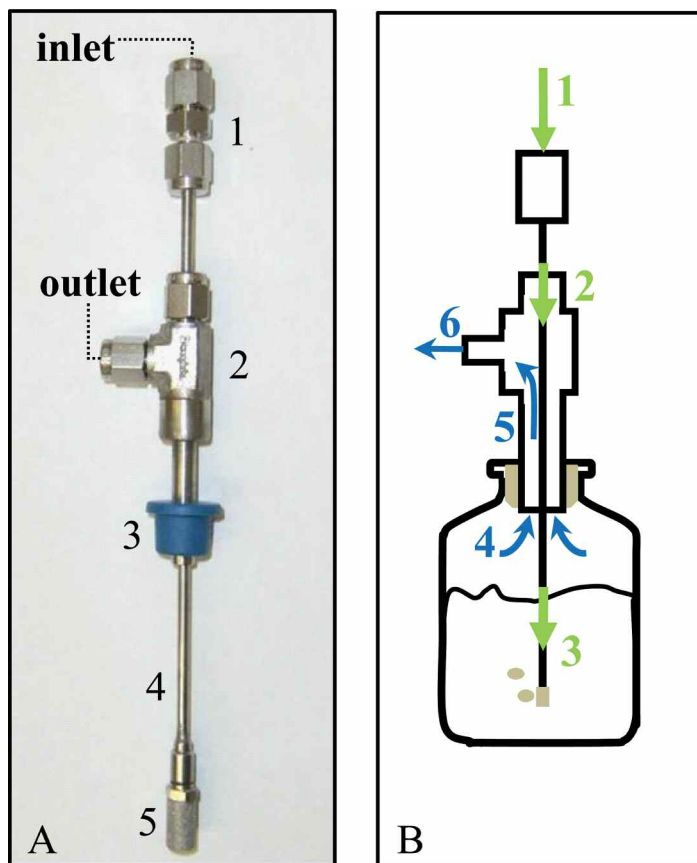

Fig. 3. Part A, photograph of a stripping probe: (1) Swagelok tube fitting union, 1/8-inch tube OD, (2) modified Swagelok female run tee (316 stainless steel, 1/8-inch OD tube fitting × 1/8-inch female NPT pipe fitting × 1/8-inch OD tube fitting, the tee was bored through between the top tube fitting and female NTP pipe fitting to accommodate 1/8-inch OD tubing and a 1-1/4-inch piece of 316 stainless steel 1/4-inch OD tubing was welded to the female NTP pipe fitting) with blue septa (Grace #6512) placed in the tube fittings, (3) cored blue butyl stopper (Bellco Glass # 2048-11800), (4) 316 stainless steel tubing, 1/8-inch tube OD with a 10-32 thread female nut welded to the bottom, (5) sintered stainless steel frit (Clayton Controls #15070) with male 10-32 thread, threaded in the female nut above. Part B, diagram of gas flow through stripping probe and sample: (1) nitrogen is introduced to the inner section of the stripping probe; (2) the nitrogen flows down the inner section of the stripping probe; (3) the nitrogen flows through the stripping probe frit, bubbles through the sample water, and strips the dissolved gasses to the sample headspace; (4) the headspace flows into the outer section of the stripping probe; (5) the headspace flows up the outer section of the stripping probe; (6) the headspace flows out of the stripping probe. Stripping probes were rinsed with 5% hydrochloric acid, dionized water, and methanol and air dried between samples.

sparging began. During sample sparging, the pressure in the vacuum line needs to be low enough to sufficiently freeze down CO_2, but still high enough to allow reasonable flow rates for sample sparging and prevent sample water from being pulled into the vacuum line. Thus, the N_2 flow and vacuum were balanced (using valves 1 and 14) to create a steady line pressure of 80-100 mtorr with a ca. 5 mL min^{-1} flowrate. Sample sparging was allowed to continue for 20 min to ensure

that all CO_2 was stripped from the sample and trapped in the vacuum line. The sparging period was concluded by turning off the N_2 flow at the flowmeter, allowing the line pressure to pump down to 50 mtorr, closing the sample valve (8), and then evacuating the residual N_2 from the vacuum line (8-14).

Quantification of the extracted CO_2 (Step D)

The CO_2 trap (11) was isolated and a dry ice-ethanol bath was placed on the trap to retain residual water. Three minutes after placing the dry ice bath, the sample CO_2 was transferred to a calibrated volume (12) with a pressure gauge (13) and quantified. The amount of CO_2 recovered and the measured mass of the sample were used to calculate the DIC concentration (ΣCO_2) of the seawater sample.

Reduction to graphite and AMS measurement (Step E)

The CO_2 extracted from natural samples was graphitized using a sealed tube zinc reduction method (Xu et al. 2007) and analyzed for ^{14}C-content at the Keck Carbon Cycle AMS (KCCAMS) facility at UC Irvine (Southon and Santos 2004, 2007). The CO_2 extracted from labeled samples was flame sealed in 6 mm Pyrex tubes and set aside for dilution.

Labeled CO_2 dilution

The amount of dilution required to bring the ^{14}C-content of each labeled sample within the AMS detection limit was estimated using oxidation rates provided by parallel ^{3}H-CH_4 RT rate measurements (see "*Assessment: Proof of concept*"). Then, dilutions were performed by mixing the sample CO_2 with an appropriate amount of ^{14}C-free CO_2. A careful record of the mixing ratios was kept by mixing in a calibrated volume with a pressure gauge (Fig. 2, #12-13). The ^{14}C-diluted CO_2 was reduced to graphite and its ^{14}C-content measured as described above. Finally, the ^{14}C content of the pre-diluted labeled CO_2 was back calculated using the recorded mixing ratios and AMS data in an isotope mass balance equation.

Step 5: ^{14}C-cell biomass analysis

The ideal ^{14}C-cell biomass analysis would involve filtering out cells from samples in the field before samples are killed with NaOH, and such a method is described below in the "*Comments and recommendations*" section. However, for the data presented here, samples were not filtered shipboard, were killed with NaOH (final pH~10), and stored > 2 mo before analysis. In genetic studies, the use of NaOH to help break down cell walls is common (Birnboim and Doly 1979). Thus, the long sample storage period with NaOH likely lysed the methanotroph cells and undermined the utility of filtration back in a land-based laboratory. As a result, we quantified the ^{14}C incorporated in the cell biomass by measuring the ^{14}C-content of the total organic carbon (TOC) in our labeled samples.

TOC is generally comprised of two pools: particulate organic carbon (POC, which contains the cell biomass) and dissolved organic carbon (DOC). The cells in our basified samples likely lysed and entered the DOC pool. The ^{14}C-content of the cellular remains was far greater than the ^{14}C-content of the background TOC, so we can assume that all (>99%) of the ^{14}C-TOC measured originated from the ^{14}C-labeled cells and back-

ground ^{14}C-DOC did not significantly contribute. Note that methanotroph cells can excrete fixed ^{14}C as DOC (methanol or other organic compounds; Bussmann et al. 2006; Costa et al. 2001; Hanson and Hanson 1996). While a small portion of this excreted ^{14}C-DOC may have been removed with other volatile compounds during stripping of the unreacted CH_4 and sample drying for ^{14}C-TOC analysis (see next paragraph), the bulk of it likely remained and influenced our ^{14}C-TOC measurements. Therefore, the ^{14}C-TOC measurement used here cannot distinguish between ^{14}C excreted and ^{14}C taken into the cell biomass, whereas direct filtering of cells can make this distinction. For studying carbon allocation and dynamics, this distinction is necessary, but for methane oxidation rate measurements, only the total amount of ^{14}C-CH_4 taken up is important.

We measured the ^{14}C-TOC by combusting dried sub-samples of our labeled samples in sealed quartz tubes (similar to Fry et al. 1996). Following DIC extraction, samples were vortex mixed, their stoppers removed, and 20-200 mg sample aliquots transferred to small quartz tubes (6 mm diameter, 1/2-inch length, prebaked at 900°C for 2 h) using disposable plastic pipettes. The sample aliquots were quantified by weighing the quartz tubes on a microbalance before and immediately following the sample transfer (if the sample is not weighed immediately after transfer, its weight will change due to evaporation). After weighing, the samples were dried in the oven at 50°C for 3 d in an aluminum heating block.

The dried sample tubes were removed from the oven and set inside quartz combustion tubes (9 mm diameter, 6-10-inch length, prebaked at 900°C) containing acetanilide (0.2-1 mg, weighed in pressed tin cups on a microbalance), cupric oxide (60 mg), and silver wire (ca. 3 mm, prebaked at 900°C). The dried sub-samples had high ^{14}C concentrations, but very little organic carbon (<0.0003 mg). Thus, the acetanilide acted as a dead (^{14}C-free) carbon carrier, whereas the cupric oxide supplied oxygen for combustion and the silver wire removed sulfur and chlorine compounds that can interfere with graphitization. The tube assemblies were evacuated, flame sealed, combusted at 900°C for 2 h, and the sample TOC and acetanilide were burned to CO_2. Following combustion, the CO_2 was extracted from the tube assemblies, quantified, converted to graphite, and analyzed for ^{14}C following the methods of Xu et al. (2007).

Step 6: Rate calculations

The increase in the ^{14}C-content of the DIC ([14]$C_{\text{DIC increase}}$) and the cell biomass ([14]$C_{\text{Cell increase}}$) during sample incubation with ^{14}C-CH_4 tracer was calculated as shown in Eqs. 3 and 5, respectively, using data obtained from the analyses described in "*Step 4: ^{14}C-DIC analysis*" and "*Step 5: ^{14}C-Cell biomass analysis.*"

$$^{14}C_{\text{DIC increase}} = [\,^{14}C_{\text{LS}} - \,^{14}C_{\text{NS}}] \times DIC \times V_s \qquad (3)$$

$$^{14}C_{\text{TOC Total sub-sample}} = \,^{14}C_{\text{Measured}} \times C_{\text{Recovered}} \qquad (4)$$

$$^{14}C_{\text{Cell increase}} = [^{14}C_{\text{TOC Total sub-sample}} \times M_{\text{Sample}}]/M_{\text{Sub-sample}} \quad (5)$$

In Eq. 3, $^{14}C_{\text{LS}}$ is the $^{14}C/^{12}C$ ratio of the labeled sample DIC, $^{14}C_{\text{NS}}$ is the $^{14}C/^{12}C$ ratio of the natural sample DIC, DIC is the DIC sample concentration in moles carbon per liter sample, and V_s is the sample volume. In Eqs. 4 and 5, $^{14}C_{\text{Measured}}$ is the $^{14}C/^{12}C$ ratio of the TOC in the dried/combusted sub-sample, $C_{\text{Recovered}}$ is the moles of CO_2 recovered from the combustion of the dried sub-sample with acetanilide, $M_{\text{Sub-sample}}$ is the mass of the sub-sample, and M_{Sample} is the mass of the original seawater sample. The $^{14}C_{\text{Measured}}$ in Eq. 4 is the $^{14}C/^{12}C$ ratio of the sub-sample TOC because the ^{14}C contribution from the acetanilide dead carbon carrier was subtracted during blank corrections to the raw ^{14}C-AMS data.

$$F_{14C} = [^{14}C_{\text{DIC increase}} + {}^{14}C_{\text{Cell increase}}]/^{14}C\text{-}CH_{4 \text{ tracer}} \quad (6)$$

$$k = F_{14C}/t \quad (7)$$

$$\tau = 1/k \quad (8)$$

$$R = k \times [CH_4] \quad (9)$$

Methane oxidation rates (R) and turnover times (τ) were calculated as shown in Eqs. 6-9 using the results from Eqs. 3 and 5 along with the ^{14}C-CH_4 tracer activity, incubation duration (t), and ambient methane concentrations ($[CH_4]$). Ambient CH_4 concentrations were measured in parallel with oxidation rate samples and the data are presented in Mau et al. (unpub. data) and Heintz (2011). In Eqs. 6-9, ^{14}C-$CH_{4 \text{ tracer}}$ is the moles of ^{14}C tracer injected, F_{14C} is the fraction of the injected ^{14}C-CH_4 that was incorporated into the oxidation products, and k is the fractional turnover rate.

Activity of the ^{14}C-CH_4 tracer

In this section, we cover the techniques used to quantify the activity concentration of our low-level ^{14}C-CH_4 tracer. The activity falls at the minimum detection limit for standard decay-counting techniques, but above the AMS maximum detection limit. Therefore, we diluted aliquots of tracer (20-40 µL) in 16 L of ^{14}C-free CH_4 in pre-evacuated 6 L stainless steel gas canisters, measured the ^{14}C-content of the diluted tracer by AMS, and back calculated the activity concentration. The canister volumes were approximately 6 L, so the amount of ^{14}C-free CH_4 added to each canister was quantified by weighing the canister prior to and following the addition of the ^{14}C-free CH_4. The mass of the ^{14}C-free CH_4 was converted to a volume using the molar mass of CH_4 and the ideal gas law, and a volume-to-volume mixing ratio was calculated for the dilution.

An aliquot of the diluted ^{14}C-CH_4 tracer was then prepared for AMS analysis using a continuous flow vacuum line (Fig. 4; numbers in parentheses below refer to numbers in this figure) adapted from Kessler and Reeburgh (2005) and Valentine et al. (2001). The procedure involves combusting the ^{14}C-CH_4 to CO_2 and water in a furnace, cryogenically purifying and trap-
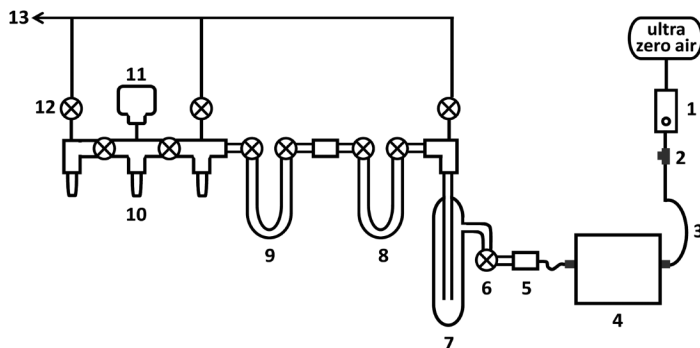

Fig. 4. Methane combustion line: (1) flowmeter (0-500 mL min⁻¹), (2) Swagelok tube fitting union tee (1/8-inch tube OD) with blue septum for injection, (3) polypropylene tubing, 1/8-inch tube OD, (4) Lindberg/Blue Furnace (Thermo Scientific #TF55050A) at 975°C with a 316 stainless steel combustion tube (1/2-inch tube OD) filled with cupric oxide to provide oxygen for combustion, (5) Swagelok Ultra-Torr 1/4-inch union with tube fitting adapter (1/4-inch tube stub × 1/8-inch OD tubing fitting) and polypropylene tubing, (6) sample valve: stem vale separating the furnace from the vacuum line, (7) water trap cooled with dry ice-ethanol slush, (8) water trap with glass beads cooled with dry ice-ethanol slush, (9) CO_2 trap with glass beads cooled with LN_2, (10) calibrated volume, (11) Baratron (MKS Inst.) digital pressure gauge, (12) vacuum valve: plug valve that separates the vacuum line from the vacuum pump, (13) vacuum pump, and (⊗) valve.

ping the CO_2 product, quantifying the recovered CO_2, reducing the CO_2 to graphite, and measuring the ^{14}C-content by AMS. Before each analysis, dry ice-ethanol baths were placed on the water traps (7 and 8) and the entire vacuum line (1-12) was flushed with ultra-zero air and evacuated 3 times. Then, a continuous flow of gas through the line (1-12) was created by introducing a ca. 5 mL min⁻¹ flow of ultra-zero air at the flowmeter (1) and opening the vacuum valve (12). The airflow and vacuum quickly balanced to create a line pressure (read at 11) of ca. 3 mtorr and a Dewar of LN_2 was placed on the CO_2 trap (9).

Next, the diluted ^{14}C-CH_4 tracer was introduced to the vacuum line by filling a gas tight Hamilton syringe (previously flushed with dilute ^{14}C-CH_4) with 3 mL diluted tracer, venting the syringe to 2 mL, and then slowly injecting the diluted tracer into the line through the injection port (2). The diluted tracer flowed with the ultra-zero air through the 975°C furnace (4) and was combusted to CO_2 and water. The CO_2/water/air mixture then flowed through two dry ice-ethanol cooled traps (7 and 8), and the water was removed. The purified CO_2/air mixture flowed through a LN_2 cooled trap (9) and the CO_2 froze down while the air was pumped away. This process was allowed to continue for 10 min to ensure that all of the injected ^{14}C-CH_4 was combusted and trapped. After 10 min, the air flow was turned off, the traps (7-9) were isolated from the furnace (4) by closing the sample valve (6), and the residual ultra-zero air was evacuated from the traps. The purified CO_2 was quantified, reduced to graphite, and its ^{14}C-content measured as described in the "*^{14}C-DIC Analysis*" section. Finally, the

activity of the ^{14}C-CH$_4$ tracer was back calculated using the volume-to-volume mixing ratio from dilution and the ^{14}C-AMS data in an isotope mass balance equation.

Assessment

A series of experiments were conducted to test the efficiencies, blanks, and precision associated with the ^{14}C-CH$_4$ LLRT method. The experiments and results are described below and summarized in Table 3. AMS results are reported in $\Delta^{14}C$ (‰) or fraction modern (FM) as defined in Stuiver and Polach (1977). As a proof of concept, we compare parallel methane oxidation rate measurements made using the ^{14}C-CH$_4$ LLRT method described here and a previously published ^3H-CH$_4$ RT method (Valentine et al. 2001).

^{14}C-labeling of samples

The precision of the ^{14}C-CH$_4$ activity is addressed in "*Activity of the ^{14}C-CH$_4$ tracer.*" Here, the accuracy and precision of the tracer volume (50 µL) were assessed by dispensing 50 µL aliquots of MilliQ water into 1 mL vials with septum using the same Hamilton syringe that was used for treating samples with the ^{14}C-CH$_4$ tracer. The 1 mL vials were weighed before and following the addition of MilliQ water and the volume of injected water was calculated using the water mass and density. The Hamilton syringe, with reproducibility adapter set at 50 µL, dispensed 49.21 ± 0.23 µL with a precision of 0.48%.

^{14}C-DIC analysis

First, the total carbon blank of the continuous flow vacuum line used to extract DIC (hereafter referred to as the extraction line) was tested by extracting DIC from 60 mL acidified, degassed, MilliQ water following the extraction procedures outline above. The total carbon line blank is 0.004 ± 0.001 mg carbon per 60 mL water ($n = 2$), which is 0.2% of the average

1.70 mg carbon that we collect per 60 mL of seawater.

Second, the ^{14}C-blank and efficiency of the extraction line were tested using ^{14}C-free spar calcite ground to a fine powder. Aliquots of spar calcite (14.7-16.7 mg) were weighed out and stored in vials with rubber stoppers (Kendall Healthcare #8881 301215), and later transferred to stripped seawater in a CO_2-free atmosphere. The transfer occurred as follows: a calcite vial (with stopper removed) and stripped seawater sample (with stripping probe still in place) were set inside a loosely enclosed chamber, and the chamber was flushed with UHP N_2 for 5 min. Then, with N_2 still flowing, the stripping probe was removed from the sample bottle, the calcite was poured into the bottle, and the stripping probe was quickly returned. Once the calcite was transferred to the seawater, it was treated as a normal sample and subjected to the DIC extraction procedures outlined above. The extraction line efficiency was calculated by comparing the amount of CO_2 extracted to the amount of calcite weighed out and found to be 99.1 ± 2.2% ($n = 8$). The average $\Delta^{14}C$ of the extracted CO_2 (the ^{14}C-line blank) was –995.2 ± 1.2‰ ($n = 8$).

Third, the accuracy and precision of the DIC extraction line were tested using duplicates of seawater samples that were previously analyzed in Ellen Druffel's Lab at UC Irvine for ^{14}C-DIC and DIC concentration (ΣCO_2, results reported in Hinger et al. 2010 and listed here in Table 4). We analyzed the duplicate samples using the procedures outlined above, and our results (Table 4) show a pooled standard deviation of 1.8‰ (2.9‰ taking the larger difference in the DIC I 2/14/07 pair into account) and are not statistically different from the previous measurements.

Last, the precision of the ^{14}C-DIC measurement of labeled and natural samples that were subject to the shipboard proce-

Table 3. Summary of the efficiencies, blanks, and precisions associated with the ^{14}C-DIC, ^{14}C-TOC (cell), and ^{14}C-CH$_4$ analyses.

Analysis	Total carbon blank (mg carbon)	^{14}C blank (‰)	Efficiency (%)	Precision*
^{14}C-DIC	0.004 ± 0.001	–995.2 ± 1.2	99.1 ± 2.2	3.7‰ natural DIC
				1.9 % labeled DIC
^{14}C-TOC (cell)	—	–982.9 ± 2.3	101.3 ± 2.8	14.8%
^{14}C-CH$_4$	0.0071 ± 0.0029	–991.4 ± 1.5	102 ± 2	0.90%

*All precisions were calculated from duplicates analyses as described in the "*Assessment*" section.

Table 4. DIC concentration (ΣCO_2) and $\Delta^{14}C$-DIC data for duplicate seawater samples from Ellen Druffel's Lab at UC Irvine. The Duffel Lab results are listed under "expected," whereas the results from our analyses of the duplicate samples are listed under "mean."

Sample name	n	DIC expected* (mol/L × 10⁻³)	DIC mean (mol/L × 10⁻³)	± 1σ	$\Delta^{14}C$ expected* (‰)	$\Delta^{14}C$ mean (‰)	± 1σ
DIC II 9/14/06	3	2.08	2.04	0.07	32.2	30.6	1.7
DIC II 10/17/06	1	2.04	2.07	—	33.7	31.2	—
DIC I 2/14/07	2	2.07	2.15	0.01	48.4	42.7	1.8
DIC II 12/6/07	4	2.01	2.03	0.03	25.0	25.4	1.9

*The expected values are published in Hinger et al. (2010). The precision of the expected DIC values is ± 0.041 × 10⁻³ mol/L, while the precision for the $\Delta^{14}C$ is ± 2‰.

dures described previously (labeling, incubating, killing, sparging) was assessed. The precision associated with natural samples is ± 3.7‰ and was determined by pooling the standard deviations in 7 sets of duplicate samples. The precision associated with labeled samples differs from the natural samples because of the dilution procedure used for samples. The CO_2 from 13 labeled samples ranging from 1.4-400 FM was split and diluted in parallel, and the precision was calculated by averaging the coefficients of variation for each sample pair and found to be 1.9%.

^{14}C-cell biomass analysis

The blank, precision, and efficiency of the dry combustion ^{14}C-TOC method used to quantify the ^{14}C uptake in cell biomass were tested. The ^{14}C-blank was determined by drying and combusting 20-200 mg aliquots of natural seawater with ~0.3 mg acetanilide as outlined above and found to be –982.9 ± 2.3‰ ($n = 4$). This blank stems from two sources: carbon contaminants on the pressed tin cups used to weigh out and hold the acetanilide, and CO_2 absorbed by the sample quartz tubes during the 3-d seawater drying period. The blank and its error were incorporated into the ^{14}C-AMS data during routine analysis of the raw data. The precision of the method by sub-samples run in parallel is 14.8% (averaged coefficients of variation from 16 pairs of duplicate sub-samples). The method combustion efficiency was evaluated by comparing the CO_2 recovered to the mass of the acetanilide added and found to be 101.3 ± 2.8%. Only 20-200 mg of ^{14}C-labeled seawater containing < 0.0003 mg carbon were dried for combustion with acetanilide. This amount of carbon is below our detection limit, so the contribution of the sample organic matter to the recovered CO_2 could not be determined.

Activity of the ^{14}C-CH$_4$ tracer

First, the total carbon blank of the vacuum line used to prepare aliquots of diluted ^{14}C-CH$_4$ for AMS analysis (hereafter referred to as the combustion line) was determined by injecting N_2 into the line and treating it as a normal CH_4 sample. The total carbon line blank is 0.0071 ± 0.0029 mg carbon ($n = 9$), which is 0.71% of the 1 mg carbon usually collected from a sample. Second, the combined ^{14}C-blank of the combustion line and dilution procedure (used to dilute the ^{14}C-CH$_4$ tracer for AMS analysis) was assessed using aliquots of ^{14}C-free CH_4 stored in a 6 L gas canister (the same type of canister used for the ^{14}C-CH$_4$ tracer dilutions). Aliquots of the ^{14}C-free CH_4 were removed from the canister and prepared for AMS using the combustion/purification procedures outlined above. The ^{14}C procedural blank is –991.4 ± 1.5‰ ($n = 7$), and this includes impurities gained during tracer dilution and sample preparation for AMS on the combustion line. Note that the above blanks can only be achieved after the tube furnace is baked out for 1-2 d at 990°C with a 20 mL min^{-1} ultra-zero airflow. Third, the efficiency of the combustion line was tested by comparing the volume of injected CH_4 (2 mL) to the amount of CO_2 recovered and found to be 102 ± 2% ($n = 22$). Last, the combined precision of the combustion line and dilution procedure

was found to be 0.90% ($n = 9$) by comparing the activity of the ^{14}C-CH$_4$ tracer determined from different canisters of diluted ^{14}C-CH$_4$ tracer. This translates to an error of ± 2.6 for the 292 Bq mL^{-1} activity concentration of the ^{14}C-CH$_4$ tracer, and combining the Hamilton syringe and activity concentration precisions using error propagation equations shows that we added 14.6 ± 0.2 Bq of ^{14}C-CH$_4$ to each sample.

Killed controls

The purpose of a killed control is to ensure that the ^{14}C-CH$_4$ tracer is not incorporated into a sample by nonbiological processes, and to test for impurities in the ^{14}C-CH$_4$ that may stay behind after sparging. During sample collection, at every tenth sampling depth, an extra bottle of seawater was collected for a killed control: a sample that was killed before or just after inoculation with ^{14}C-CH$_4$. After killing and inoculation, killed controls were treated as normal samples, incubated, sparged, and returned to the laboratory for ^{14}C-AMS analysis. There was ~30 min delay between injection and killing of our killed control samples because killing was carried out inside a N_2 filled glove bag and purging and inflating the glove bag took time. The one killed control we analyzed had a rate ~8% of its corresponding rate sample, and this showed that a small amount of oxidation took place during the delay. We also processed several killed control samples that were killed with sodium azide ~1 h before the injection of ^{14}C-CH$_4$. The ^{14}C-DIC values from these killed controls (–173.6‰ and –18.8‰) show no signs of unintended incorporation or impurities because they are consistent with their respective natural samples.

Overall performance

Combining the above precision values and others not listed here (balances, calibrated volume, ext.) into the oxidation rate calculations (Eqs. 3-9) using error propagation equations yields an overall precision of 5.3% for the ^{14}C-CH$_4$ LLRT oxidation rate values reported here (excluding rates < 0.00025 nM d^{-1}). This propagated error is slightly more than the 4.7% precision determined by averaging the coefficients of variation from 5 pairs of duplicate rate measurements. The largest part of the propagated error results from the ^{14}C-TOC (Cell) measurement (avg. 65%), followed by the ^{14}C-DIC (avg. 16%), ^{14}C-CH$_4$ tracer (avg. 12%) and methane concentration (avg. 6%) measurements, and finally the incubation time (avg. 1%).

At slower rates, the ^{14}C-DIC and ^{14}C-cell biomass in the labeled samples approaches that of the natural samples and the method precision begins to degrade. If a 20% precision (based on propagated error) is chosen as the maximum desired error, then the LLRT method presented here can measure turnover times up to 57 y. The precision of the ^{3}H-CH$_4$ RT method based on average coefficients of variation from duplicate rate measurements is 16% (Heintz 2011) and its detection limit (choosing a 20% error limit) based on error propagation calculations is 11 y. The detection limits reported here for both rate measurement methods will change with experimental conditions (e.g., tracer activity concentration, sample size,

counting volume, etc.), and are especially dependent on the maximum desired error and amount of tracer added to each sample.

Proof of concept: Parallel rate measurements

Water samples were collected as described above aboard the R/V *Atlantis* during the SEEP's 07 Cruise to the Santa Barbara and Santa Monica Basins, 3-17 July 2007. As a proof of concept, parallel oxidation rate measurements were made using the ^{14}C-CH$_4$ LLRT method and a previously published ^{3}H-CH$_4$ RT method (*see* Valentine et al. 2001 for method details; ^{3}H-CH$_4$ rate data are reported in Heintz 2011 and Mau et al. unpub.
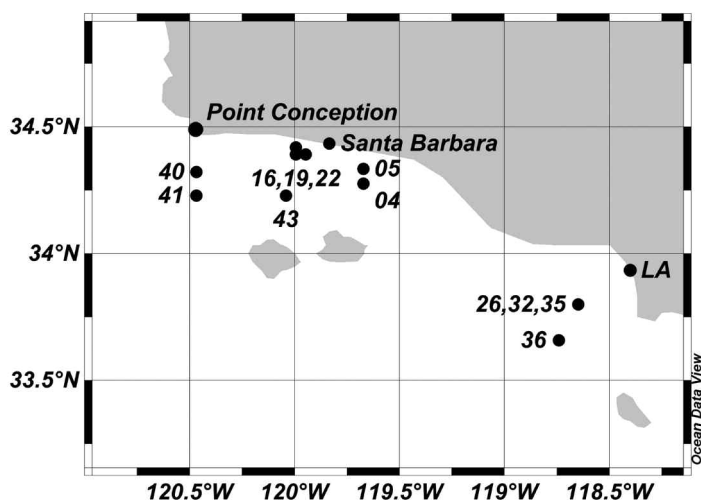

Fig. 5. Location of study area off the coast of southern California, USA. CTD casts are shown as black circles and labeled by number.
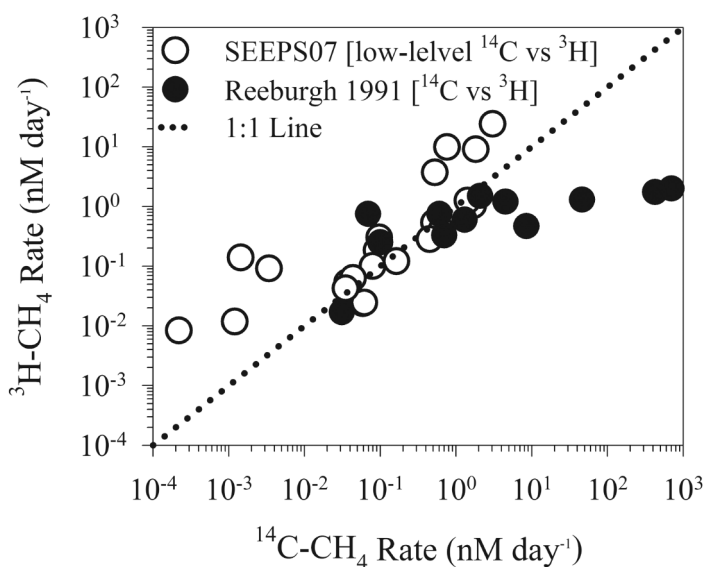

Fig. 6. Correlation of rates within two sets of parallel methane oxidation rate measurements. The open circles show correlation between the ^{3}H-CH$_4$ RT and ^{14}C-CH$_4$ LLRT parallel rate measurements presented here. The closed circles show correlation between the ^{3}H-CH$_4$ and ^{14}C-CH$_4$ RT rate measurements presented in Reeburgh et al. (1991).

data) with water from the same Niskin bottles at 12 stations (Fig. 5). The parallel measurements are generally consistent and have a correlation coefficient of 0.77 (Fig. 6, Table 5). However, the measurements do contain a number of mismatches that concentrate at slower rates and that result in the LLRT ^{14}C rates being 0.4-98 times slower than the ^{3}H rates. Reeburgh et al. (1991) made parallel oxidation rate measurements in the Black Sea water column with existing ^{3}H-CH$_4$ and ^{14}C-CH$_4$ RT methods and found a similar correlation coefficient of 0.73 (Fig. 6). Reeburgh and coworkers' parallel measurements also contained mismatches, but their ^{14}C rates were 0.1-350 times faster than their ^{3}H rates. The parallel rates from each of the 12 stations that we occupied were combined and plotted on depth profiles for the Santa Barbara and Santa Monica Basins (Fig. 7). Despite the mismatches, the trends in the ^{14}C-CH$_4$ LLRT and ^{3}H-CH$_4$ RT rates (referred to as LL ^{14}C and ^{3}H rates below) match well through these depth profiles. Below, we discuss potential causes of the parallel rate mismatches.

First, several LL ^{14}C samples were incubated at temperatures different than the parallel ^{3}H samples due to limited incubators in the shipboard radioisotope facilities. The metabolic rate of

Table 5. Methane oxidation rates from the ^{3}H-CH$_4$ RT and ^{14}C-CH$_4$ LLRT parallel rate measurements made during the SEEPS 07 cruise. The LL ^{14}C rates containing two entries are duplicate measurements. The ^{3}H rates are reported in Heintz 2011 and Mau et al. (unpubl. data).

| Sample cast #	Depth (m)	LL ^{14}C rate (nM/d)	^{3}H rate (nM/d)
Santa Barbara Basin			
4	139	0.037	0.054
5	10	0.0034	0.092
16	11	0.0014	0.14
19	31	0.76	9.9
19	51	3.0	24
22	50	0.52	3.7
22	70	1.8	9.1
22	91	1.6, 1.8	1.0
41	200	0.097	0.30
41	350	0.51	0.54
43	202	0.089	0.19
43	350	0.076, 0.082	0.10
43	578	1.4, 1.5	1.3
Santa Monica Basin			
26	796	0.64	0.40
32	401	0.00021, 0.00023	0.0084
32	701	0.044, 0.043	0.063
35	450	0.0012	0.012
35	600	0.059	0.024
35	642	0.062	0.025
35	680	0.035	0.043
36	700	0.45	0.28
36	800	0.16	0.12
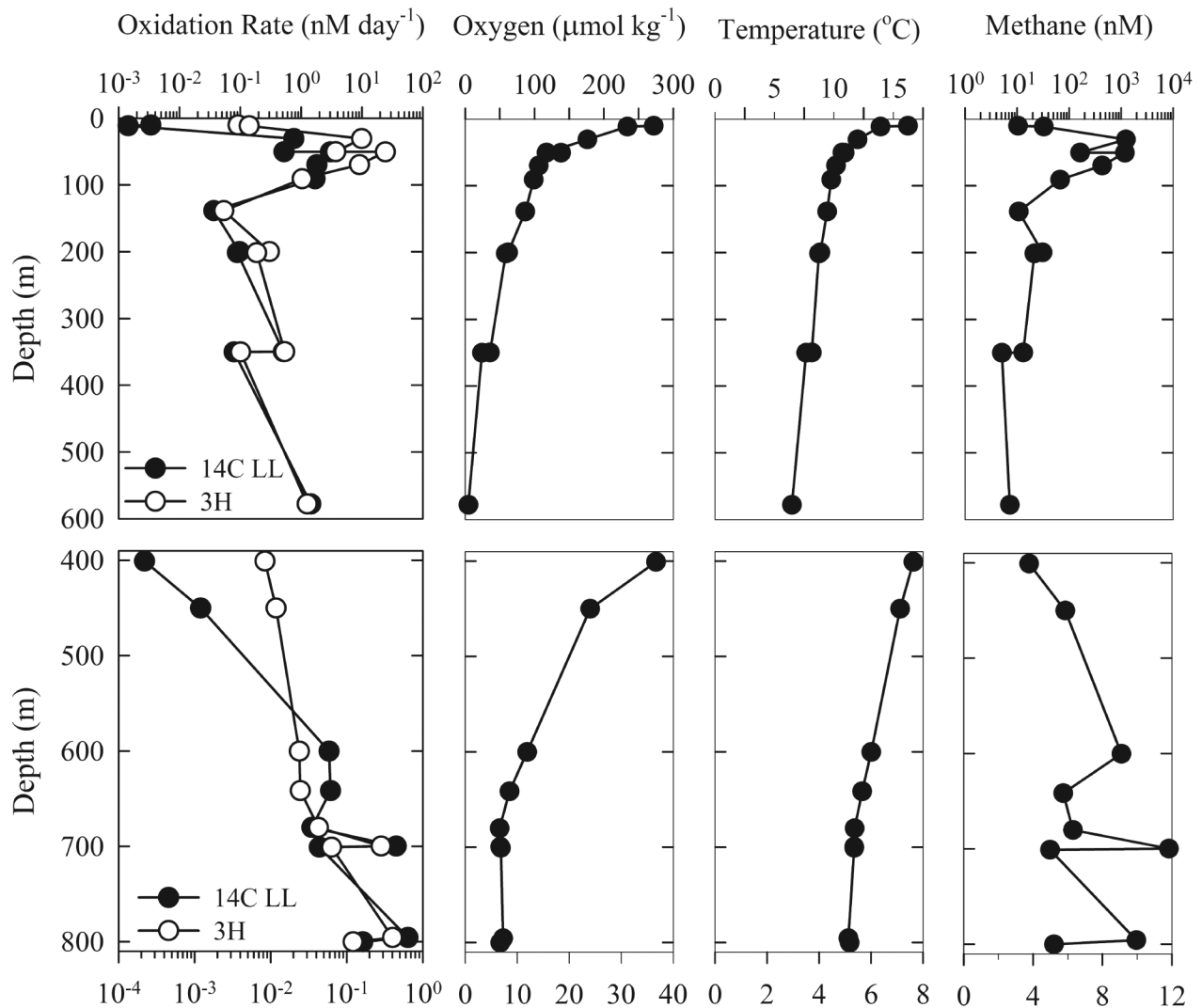
Fig. 7. Profiles of the ^{14}C-CH$_4$ LLRT and ^{3}H-CH$_4$ RT parallel rate measurements and the accompanying chemical and hydrographic parameters for the Santa Barbara Basin (top) and the Santa Monica Basin (bottom). Error bars for both sets of rate measurements fall with the data point symbols.

methanotrophs, as with all organisms, is sensitive to temperature (Gillooly et al. 2001; Hanson and Hanson 1996; Heintz 2011), so the incubation temperature differences may have contributed to the mismatches in the parallel rate measurements. Our data shows that LL ^{14}C samples yield slower rates than the parallel ^{3}H samples when they are incubated at colder temperatures and vice versa (Fig. 8). Correcting the LL ^{14}C rates using a Q$_{10}$ temperature coefficient can resolve some of the mismatches in the parallel measurements. For example, the LL ^{14}C sample at 139 m in Cast 4 was incubated at 6°C whereas the parallel ^{3}H sample was incubated at 9°C. If a Q$_{10}$ of 2.2 (median of the range from Gillooly et al. 2001; Hanson and Hanson 1996; Heintz 2011) is used to correct the LL ^{14}C rate to 9°C, the rate increases from 0.037 to 0.047 nM CH$_4$ d^{-1} and agrees with the parallel ^{3}H rate of 0.054 nM CH$_4$ d^{-1}. However, if a similar correction is applied to the LL ^{14}C sample at 10 m in Cast 5 (6°C to 12°C temperature correction), the rate only
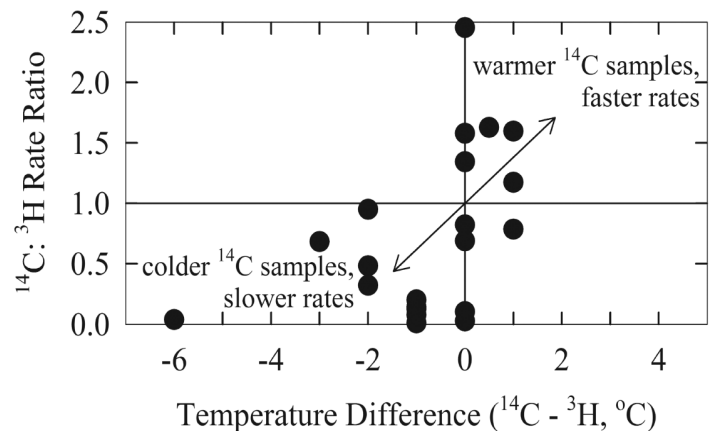

Fig. 8. Plot demonstrating the relationship between incubation temperature differences (LL ^{14}C temp. – ^{3}H temp.) and mismatches in the ^{3}H-CH$_4$ RT and ^{14}C-CH$_4$ LLRT parallel rate measurements.

increases from 0.0039 to 0.0062 nM CH_4 d^{-1} and is still an order of magnitude lower than the 0.092 nM CH_4 d^{-1} ^3H rate.

Second, priming may have played a role in the parallel rate mismatches. The ^3H method used here increased the sample CH_4 by 12.5 nM whereas the LL ^{14}C method added only 0.4 nM of CH_4 (30 times less). Methane concentrations in our samples ranged from 3.8-1237 nM, so the ^3H method significantly influenced ambient CH_4 concentrations (up to 329% increase) in our least concentrated samples. Methane oxidation rates are dependent on CH_4 concentration (Ward et al. 1987), so CH_4 additions may prime the methanotroph community and cause mistakenly high rates. Priming may have affected previous RT oxidation rate measurements (e.g., Jones 1991; Ward 1992), and many studies using the existing ^{14}C-CH_4 RT methods have addressed the issue by making duplicate rate measurements with increasing CH_4 additions, identifying the relationship between CH_4 concentration and oxidation rate (usually linear), and extrapolating back to in situ CH_4 concentrations (e.g., Reeburgh et al. 1991; Ward 1992; Ward et al. 1987). Ward et al. (1987) made such measurements on duplicate oxic water samples and found a linear relationship with a slope of 1.8×10^{-5} (nM CH_4 d^{-1}) nM^{-1} CH_4. The linear relationship predicts a 0.00023 nM CH_4 d^{-1} rate increase for a 12.5 nM addition of CH_4. Appling this correction (to compensate for priming in ^3H samples) to our LL ^{14}C oxidation rates ranging from 0.00021 to 3.4 nM CH_4 d^{-1} increases the rates by a factor of 1.001 to 2.1. Therefore, priming was likely an important factor in the slower parallel rate mismatches, but not the faster ones.

One mechanism behind the priming effect is enzyme level kinetics. Methanotrophs mediate the first step in methane oxidation with an enzyme named methane monooxygenase (MMO; Murrel et al. 2000), and the kinetics of this enzyme can be approximated with the Michaelis-Menten kinetic model. According to the model, oxidation rates will increase hyperbolically with methane concentration until the MMO enzyme becomes saturated and oxidation rates reach a maximum value. The Michaelis-Menten equation that describes this hyperbolic increase relates methane concentration to oxidation rate using the parameters Vmax (maximum oxidation rate) and Ks (1/2 saturation constant). We estimated the potential magnitude of this effect by using kinetic parameters (Vmax and Ks) experimentally determined by Ward and Kilpatrick (1990) (Fig. 5, Table 1), our samples' ambient CH_4 concentrations, and the 0.4 and 12.5 nM CH_4 increase caused by the LL ^{14}C-CH_4 and ^3H-CH_4 tracers, respectively, in the Michaelis-Menten equation. We calculated two sets of theoretical rates (one for each method) over the range of methane concentrations present in our samples. Then, we compared the two sets of theoretical rates and found that the 30 times more CH_4 added with the ^3H tracer can increase observed rates by 1.001-3.79 times compared with LL ^{14}C tracer. Baani and Liesack (2008) identified a MMO isozyme that only becomes active at low methane concentrations (<450-600ppm), when

MMO is not fully expressed. The kinetics of the MMO isozyme are somewhat different from MMO (it has a high affinity for CH_4), and this could have influenced our oxidation rate measurements in low methane samples.

Last, differences in the LL ^{14}C and ^3H method detection limits may have contributed to the mismatches observed in the parallel rate measurements. As outlined above, the ^3H and LL ^{14}C rate measurements can detect turnover times up to 11 and 57 y, respectively, with a maximum error of 20%. The longest ^3H turnover time measured here was 1.2 y (Cast 32, 400 m, 0.0084 nM d^{-1}) and is far away from the 11 y ^3H-CH_4 detection limit. Thus, it seems unlikely that detection limits are an issue with these data.

Overall, the mismatches in the parallel oxidation rate measurements likely stem from priming effects and incubation temperature differences. However, more parallel rate measurements in low-methane (slow turnover) environments with close attention to incubation temperatures and in the lab using duplicate water samples with increasing additions of methane (priming tests) are needed to better understand and pinpoint the source of the mismatches.

Feasibility

The two vacuum line systems presented here (Figs. 2 and 4) are modifications to a base vacuum line that would cost < $9,000 to set-up including the glassware, hardware, pressure gauge, and vacuum pump. The DIC extraction line (Fig. 2) adds a flowmeter, connective tubing, and stripping probe to the base vacuum line that would cost < $150. The CH_4 combustion line (Fig. 4) adds a tube furnace with combustion tube, flowmeter, and connective tubing to the base vacuum line costing < $2,000 (with the main cost from the tube furnace). The greatest expense associated with the procedure outlined here is the final AMS measurement costing $80-$180 or more per measurement depending on the facility used. The extraction of DIC from samples takes about 1.2 h per sample, with an added 20-30 min if the sample is labeled and requires dilution prior to AMS analysis. A set of six samples for ^{14}C-TOC analysis can be prepared in a total of 4 h spread throughout 5 d. Carrying out the procedures described herein requires basic vacuum line, heat transfer, and torch/glass blowing skills, and these skills are best learned from an experienced technician. Handling of low activity radioactive materials, compressed gas, and common chemicals (acids, bases, and alcohols) is also required and information concerning safe practices and associated hazards is available from experienced technicians, text books, and health and safety offices.

Discussion

Methane oxidation rate measurements are essential to our understanding of ocean CH_4 geochemistry; however, existing RT rate measurements are limited by strict health and safety regulations for radioactive applications (Table 1). The ^{14}C-CH_4 LLRT method described here relaxes these limitations and lays the analytic foundation for a below-regulation rate mea-

surement (see "*Comments and recommendations*"). The method uses levels of ^{14}C-CH$_4$ (292 Bq mL^{-1} with a total of 4.8×10^6 Bq in a 6L canister) that are 10^3-10^5 times lower than the existing ^{3}H-CH$_4$ (3.5-7.4×10^6 Bq mL^{-1}) and ^{14}C-CH$_4$ (1.3-4.4×10^6 Bq mL^{-1}) RT methods (Table 2) and below regulation for transportation ($<10^7$ Bq total, Table 1). Also, samples inoculated with the low-level ^{14}C-CH$_4$ tracer do not require handling as radioactive waste because they contain 0.12 Bq ^{14}C mL^{-1}, which is three orders of magnitude below the strictest regulation for liquids (296 Bq ^{14}C mL^{-1}, Table 1). The LLRT method and below-regulation methods to follow should increase sampling opportunities for methane oxidation rate measurements, and thus lead to a better understanding and quantification of the marine methane oxidation sink.

The LLRT method has another important advantage; the method increases the ambient CH$_4$ in a sample by 0.4 nM, which is 30-10^3 less than the existing RT methods (Table 2). This leads to less disruption in the microbial community and more realistic/tracer level rate measurements in low CH$_4$ areas where the previous published RT methods would overwhelm the CH$_4$ pool (e.g., 2 nM CH$_4$ open ocean water). The previously published ^{3}H-CH$_4$ and ^{14}C-CH$_4$ RT methods increase ambient CH$_4$ in a sample by 12-25 nM CH$_4$ and ~10^3 nM CH$_4$, respectively (Table 2). Because of the smaller CH$_4$ additions, the ^{3}H-CH$_4$ RT method can be used for tracer level rate measurements in medium-low CH$_4$ waters, but it cannot track carbon allocation between respiration (CO$_2$) and cell biomass. Thus, the LLRT method will be a useful new tool that can make tracer level measurement in low CH$_4$ environments and track carbon allocation.

Comments and recommendations

Low-level or below-regulation ^{14}C-CH$_4$ tracers relax the restrictions that accompany the existing-high activity RT rate measurements, but the ^{14}C-CH$_4$ tracer and labeled samples still require careful handling to avoid contamination issues with natural ^{14}C studies and AMS laboratories. Precautions that should be taken when working with tracers and labeled material are discussed here. First, work with labeled material should be isolated in designated isotope facilities both in the field and when preparing samples for AMS analysis. Second, the vacuum line used for DIC extractions should be cleaned between natural and labeled samples by exposing it to room air or water (expand a small amount of distilled water into the line) overnight. Third, samples should only be sent to AMS labs as pressed graphite and care should be taken that the graphite samples are packaged in clean materials (packing free of ^{14}C that has not been in a designated isotope facility). Graphitization can be carried out inside the designated isotope area immediately following DIC extraction using the sealed tube technique referenced here (Xu et al. 2007). Forth, frequent blanks and standards should be run to monitor memory effects. For the data presented here, ^{14}C-labeled samples, natural samples, blanks, and standards were prepared on the same

vacuum line and processed in the same AMS wheels. We saw no memory effects between samples even with ^{14}C-concentrations as high as 400 FM. If memory is seen in the vacuum line, the line can be cleaned as described above. A well-planned ^{14}C-CH$_4$ tracer-based experiment should result in samples with ^{14}C-concentrations that are < 2 FM. AMS facilities will likely not be concerned with measuring these levels of enrichment because they are similar to atmospheric concentrations following nuclear bomb testing (~1.99 FM; Levin et al. 1985). AMS preparation labs, however, will not likely accept ^{14}C-labeled samples for processing (CO$_2$ extraction and graphitization) unless they have designated isotope facilities. Thus, as mentioned above, samples will need to be sent as pressed graphite. When working with the LLRT method for the first time, we recommend that a few test samples be sent for AMS analysis before a whole batch to ensure the desired ^{14}C-levels were met. As a precaution, splits of CO$_2$ can be saved for each sample in 6-mm Pyrex flame seal tubes, so that if the samples do exceed the maximum AMS detection limit, the saved CO$_2$ can be diluted with ^{14}C-free CO$_2$ and analyzed for ^{14}C as described above.

We made three improvements to the ^{14}C-CH$_4$ LLRT rate measurement in the course of development and testing. First, we reduced the length of the post-incubation procedures by eliminating the need for a N$_2$-filled glove bag. Post incubation, a 60-mL N$_2$ headspace is introduced to the samples with the two syringe technique described above, 0.4 mL sodium hydroxide is added to the samples by syringe, and the sealed samples are sparged with UHP N$_2$ for 40 min using two needles (one 16 g, 4-inch needle inserted into the bottom of the sample bottle to deliver the N$_2$ and a 23 g, 1-inch needle inserted in the sample headspace as a vent for the stripped gasses and N$_2$ flow). After sparging, sample stoppers are replaced with blue butyl stoppers inside a loosely enclosed N$_2$ filled chamber. Second, we developed a method for filtering the cell biomass from samples in the field before the NaOH treatment for direct ^{14}C-AMS analysis. At sea, the method involves vacuum filtering 60 mL sample through a quartz fiber filter to collect cell biomass. The quartz filters are partially dried by vacuum, rolled up with tweezers, inserted into 6 mm, 2-inch prebaked quartz tubes, and completely dried on a hotplate at 60°C. Back in the laboratory, the cell biomass on the quartz filters is combusted to CO$_2$ in sealed quartz tubes and the ^{14}C-content is measured as described in "*^{14}C-Cell Biomass Analysis.*" Third, we replaced the plug value (called the vacuum valve above, Fig. 2 #14) in the DIC extraction line with a needle valve. This allows more sensitive control over the extent of vacuum used during the extraction process.

The LLRT ^{14}C-CH$_4$ oxidation rate measurement outlined here lays the analytic foundation for a below-regulation measurement. Analytic techniques for measuring oxidation rates using low-levels of ^{14}C-CH$_4$ in conjunction with AMS were identified and tested during the method's development. Now

that the analytic techniques are validated, the method can be extended to levels of ^{14}C-CH$_4$ that are below-regulation, but careful attention needs to be paid to the intended site of application. In environments where the turnover times are fast (< 400 d), the ^{14}C-CH$_4$ can be diluted below-regulation (0.037 Bq mL^{-1}, the strictest regulation for gases in Table 1) and 0.0074 Bq ^{14}C can be added per sample with 200 µL aliquots. Incubating a water sample (120 mL, 100 nM CH$_4$,) with this amount of ^{14}C-CH$_4$ for 1.5 d will increase the ^{14}C-content of the DIC by ~25 ‰ and the POC by ~1700 ‰ assuming 30% of the ^{14}C-CH$_4$ consumed is fixed to the cell biomass and the sample has a turnover time of 400 d. In environments where the turnover time is slow (>400 d), the increase in the ^{14}C-DIC will be < 25‰ and will approach the error in the ^{14}C-DIC measurement (±3.7 ‰, see above). Increasing the volume of injected ^{14}C-CH$_4$ tracer to > 200 µL to introduce more ^{14}C is not a good option because a large gas pocket in a sample may prevent the added ^{14}C-CH$_4$ from fully dissolving. To go below-regulation in these > 400 d environments, the ^{14}C-CH$_4$ will need to be delivered as a sterile aqueous solution instead of a gas. The use/possession exempt quantities for liquids are 10^3 times less strict than for gases (Table 1). Thus, a solution containing adequate ^{14}C-CH$_4$ for a rate measurement that is below-regulation could easily be made (the tracer preparation methods outlined in de Angelis et al. 1993 or Joye et al. 1999 could be adapted for this).

The ^{14}C-CH$_4$ LLRT rate measurement described here also lays the analytic foundation for many applications of below regulation ^{14}C work that take advantage of the high sensitivity of AMS. First, the method can be extended to measure methane oxidation rates in anoxic waters or sediments. For both environments, the activity of the ^{14}C-CH$_4$ tracer would need to be adjusted so that adequate ^{14}C was added to create a detectable signal in the oxidation products. In anoxic waters, the same procedures could be used as described here, but for sediments the method would need to be adapted for work with cores (e.g., Joye et al. 2004). Second, because low-level ^{14}C-CH$_4$ tracer adds small amounts of CH$_4$ yet still raises background ^{14}C concentrations in a sample significantly (natural abundance: 10^{-10} % ^{14}C versus 1% ^{13}C), the LLRT method may be used to study carbon dynamics in environments where the existing-high level ^{14}C-CH$_4$ radiotracers or ^{13}C-CH$_4$ stable isotope tracers would be impractical. For instance, a water sample could be labeled with low-level ^{14}C-CH$_4$ and the ^{14}C could be tracked through the methanotrophs, their predators, and viruses that infect the methanotrophs. Third, the LLRT method leads the way for work with other ^{14}C-labeled organic compounds at levels below-regulation. For example, the method could be adapted to measure the consumption rates of higher hydrocarbons such as ethane, propane, and butane in sediments and the water column. These hydrocarbons accompany CH$_4$ in many seep environments, and little is known about their consumption rates (Kinnaman et al. 2007; Mau et al. 2010; Valentine et al. 2010).

In conclusion, the ^{14}C-CH$_4$ LLRT method for methane oxidation rate measurements is generally consistent with the previously published ^{3}H-CH$_4$ RT method, but mismatches between methods at slower rates require further investigation. The AMS-based LLRT method compared with the decay-counting based ^{3}H-CH$_4$ and ^{14}C-CH$_4$ RT methods requires more time and funding per sample, and thus is unlikely to replace them. However, the LLRT method should prove as a useful new tool for measuring methane oxidation rates and studying carbon dynamics in low methane environments and when application of the existing RT methods is not practical (e.g., foreign venues, remote field sites, rapid response situations, etc.)

References

Alperin, M. J., and W. S. Reeburgh. 1985. Inhibition experiments on anaerobic methane oxidation. Appl. Environ. Microbiol. 50(4):940-945.

Baani, M., and W. Liesack. 2008. Two isozymes of particulate methane monooxygenase with different methane oxidation kinetics are found in *Methylocystis* sp. strain SC2. Proc. Natl. Acad. Sci. U.S.A. 105(29):10203-10208 [doi:10.1073/pnas.0702643105].

Beal, E. J., C. H. House, and V. J. Orphan. 2009. Manganese- and iron-dependent marine methane oxidation. Science 325:184-187 [doi:10.1126/science.1169984].

Birnboim, H.C., and J. Doly. 1979. A rapid alkaline extraction procedure for screening recombinant plasmid DNA. Nucleic Acids Res. 7(6):1513-1524. [doi:10.1093/nar/7.6.1513].

Blumhagen, E. D., and J. F. Clark. 2008. Carbon sources and signals through time in an alpine groundwater basin, Sagehen, California. Appl. Geochem. 23:2284-2291 [doi:10.1016/j.apgeochem.2008.03.010].

Bussmann, I., M. Rahalkar, and M. Schink. 2006. Cultivation of methanotrophic bacteria in opposing gradients of methane and oxygen. FEMS Microbiol. Ecol. 56:331-344 [doi:10.1111/j.1574-6941.2006.00076.x].

Caldwell, S. L., J. R. Laidler, E. A. Brewer, J. O. Eberly, S. C. Sandborgh, and F. S. Colwell. 2008. Anaerobic oxidation of methane: mechanisms, bioenergetics, and the ecology of associated microorganisms. Environ. Sci. Technol. 42(18):6791-6799 [doi:10.1021/es800120b].

Carini, S., N. Bano, G. LeCleir, and S. B. Joye. 2005. Aerobic methane oxidation and methanotroph community composition during seasonal stratification in Mono Lake, California (USA). Environ. Microbiol. 7(8):1127-1138 [doi:10.1111/j.1462-2920.2005.00786.x].

Carini, S. A., B. N. Orcutt, and S. B. Joye. 2003. Interactions between methane oxidation and nitrification in coastal sediments. Geomicrobiol. J. 20(4):355-374 [doi:10.1080/01490450303900].

Costa, C., M. Vecherskaya, C. Dijkema, and A. J. M. Stams. 2001. The effect of oxygen on methanol oxidation by an obligate methanotrophic bacterium studied by in vivo ^{13}C

nuclear magnetic resonance spectroscopy. J. Indus. Microbiol. Biotech. 26:9-14 [doi:10.1038/sj.jim.7000075].

Crowe, S. A., and others. 2010. The methane cycle in ferruginous, tropical Lake Matano. Geobiology [doi:10.1111/j.1472-4669.2010.00257.x].

Daniels, L., and J. G. Zeikus. 1983. Convenient biological preparation of pure high specific activity 14C-labelled methane. J. Labeled Comp. Radiopharm. 20:17-24 [doi:10.1002/jlcr.2580200104].

de Angelis, M. A., M. D. Lilley, E. J. Olson, and J. A. Baross. 1993. Methane oxidation in deep-sea hydrothermal plumes of the Endeavour Segment of the Juan de Fuca Ridge. Deep-Sea Res. I. 40(6):1169-1186 [doi:10.1016/0967-0637(93)90132-M].

Fry, B., E. T. Peltzer, C. S. Hopkinson Jr., A. Nolin, and L. Redmond. 1996. Analysis of marine DOC using a dry combustion method. Mar. Chem. 54:191-201 [doi:10.1016/0304-4203(96)00031-X].

Gillooly, J. F., J. H. Brown, G. B. West, V. M. Savage, and E. L. Charnov. 2001. Effects of size and temperature on metabolic rate. Science 293:2248-2251 [doi:10.1126/science.1061967].

Girguis, P. R., V. J. Orphan, S. J. Hallam, and E. F. DeLong. 2003. Growth and methane oxidation rates of anaerobic methanotrophic archaea in a continuous-flow bioreactor. Appl. Environ. Microbiol. 69(9):5472-5482 [doi:10.1128/AEM.69.9.5472-5482.2003].

———, A. E. Cozen, and E. F. DeLong. 2005. Growth and population dynamics of anaerobic methane-oxidizing archaea and sulfate-reducing bacteria in a continuous-flow bioreactor. Appl. Environ. Microbiol. 71(7):3725-3733 [doi:10.1128/AEM.71.7.3725-3733.2005].

Griffiths, R. P., B. A. Caldwell, J. D. Cline, W. A. Broich, and R. J. Morita. 1982. Field observations of methane concentrations and oxidation rates in the Southeastern Bering Sea. Appl. Environ. Microbiol. 44:435-446.

Hanson, R. S., and T. E. Hanson. 1996. Methanotrophic bacteria. Microbiol. Rev. 60(2):439-471.

Heeschen, K. U., R. S. Keir, G. Rehder, O. Klatt, and E. Suess. 2004. Methane dynamics in the Weddell Sea determined via stable isotope ratios and CFC-11. Global Biogeochem. Cycles. 18:GB2012 [doi:10.1029/2003GB002151].

Heintz, M. B. 2011. Rates of aerobic methane oxidation in the waters of the Santa Monica Basin and Alaskan Arctic Lakes measured with a tritium-based radiotracer technique, Ph.D. thesis. Univ. of California, Santa Barbara.

Hinger, E. N., G. M. Santos, E. R. M. Druffel, and S. Griffin. 2010. Carbon isotope measurements of surface seawater from a time-series off Southern California. Radiocarbon 52(1):69-89.

Hinrichs, K.- U., and A. Boetius. 2002. The anaerobic oxidation of methane: New insights in microbial ecology and biogeochemistry, p. 457-77. *In* G. Wefer, D. Billett, D. Hebbeln, B. B. Jørgensen, M. Schlüter, and T. C. E. van-

Weering, [eds.], Ocean margin systems. Springer-Verlag.

Hoehler, T. M., M. J. Alperin, D. B. Albert, and C. S. Martens. 1994. Field and laboratory studies of methane oxidation in an anoxic marine sediment: Evidence for methanogen-sulfate reducer consortium. Global Biogeochem. Cycl. 8(4):451-463 [doi:10.1029/94GB01800].

Jones, R. D. 1991. Carbon monoxide and methane distribution and consumption in the photic zone of the Sargasso Sea. Deep-Sea Res. 38(6):625-635 [doi:10.1016/0198-0149(91)90002-W].

Jørgensen, B. B., A. Weber, and J. Jopfi. 2001. Sulfate reduction and anaerobic methane oxidation in Black Sea sediments. Deep-Sea Res. I 48:2097-2120 [doi:10.1016/S0967-0637(01)00007-3].

Joye, S. B., T. L. Connell, L. G. Miller, and R. S. Oremland. 1999. Oxidation of ammonia and methane in an alkaline, saline lake. Limnol. Oceanogr. 44(1):178-188 [doi:10.4319/lo.1999.44.1.0178].

———, A. Boetius, B. N. Orcutt, J. P. Montoy, H. N. Schulz, M. J. Erickson, and S. K. Lugo. 2004. The anaerobic oxidation of methane and sulfate reduction in sediments from Gulf of Mexico cold seeps. Chem. Geol. 205:219-238 [doi:10.1016/j.chemgeo.2003.12.019].

Kessler, J. D., and W. S. Reeburgh. 2005. Preparation of natural methane samples for stable isotope and radiocarbon analysis. Limnol. Oceanogr. Methods 3:408-418 [doi:10.4319/lom.2005.3.408].

King, J. Y., W. S. Reeburgh, K. K. Thieler, G. W. Kling, W. M. Lova, L. C. Johnson, and K. J. Nadelhoffer. 2002. Pulse-labeling studies of carbon cycling in Arctic tundra ecosystems: The contribution of photosynthates to methane emission. Global Biogeochem. Cycl. 16:1062-1069 [doi:10.1029/2001GB001456].

Kinnaman, F. S., D. L. Valentine, and S. C. Tyler. 2007. Carbon and hydrogen isotope fractionation associated with the aerobic microbial oxidation of methane, ethane, propane and butane. Geochim. Cosmochim. Acta 71:271-283 [doi:10.1016/j.gca.2006.09.007].

Levin, I., and others. 1985. 25 years of tropospheric 14C observations in central Europe. Radiocarbon 27(1):1-19.

Mau, S., M. B. Heintz, F. S. Kinnaman, and D. L. Valentine. 2010. Compositional variability and air-sea flux of ethane and propane in the plume of a large, marine seep field near Coal Oil Point, CA. Geo-Mar. Lett. 30:367-378 [doi:10.1007/s00367-010-0185-z].

McNichol, A. P, G. A. Jones, D. L. Hutton, and A. R. Gagnon. 1994. The rapid preparation of seawater CO_2 for radiocarbon analysis at the National Ocean Sciences AMS Facility. Radiocarbon 36(2):237-246.

Moran, J. J., Beal, E. J., Vrentas, J. M., Orphan, V. J., Freeman, K. H., and C. H. House1. 2008. Methyl sulfides as intermediates in the anaerobic oxidation of methane. Environ. Microbiol. 10(1): 162-173. [doi:10.1111/j.1462-2920.2007.01441.x].

———, House, C. H., Thomas, B., and K. H. Freeman. 2007. Products of trace methane oxidation during nonmethyltrophic growth by Methanosarcina. J. Geophys. Res. 112: G02011. [doi:10.1029/2006JG000268].

Murrel, J. C., B. Golbert, and I. R. McDonald. 2000. Molecular biology and regulation of methane monooxygenase. Arch. Microbiol. 50:955-969.

Nauhaus, K., A. Boetius, M. Krüger, and F. Widdel. 2002. In vitro demonstration of anaerobic oxidation of methane coupled to sulphate reduction in sediment from a marine gas hydrate area. Environ. Microbiol. 4(5):296-305 [doi:10.1046/j.1462-2920.2002.00299.x].

Pohlman, J. W., D. L. Knies, K. S. Grabowski, T. M. DeTurck, D. J. Treacy, and R. B. Coffin. 2000. Sample distillation/graphitization system for carbon pool analysis by accelerator mass spectrometry (AMS). Nucl. Instrum. Methods Phys. Res., Sect. B. 172:428-433.

Raghoebarsing, A. A., and others. 2006. A microbial consortium couples anaerobic methane oxidation to denitrification. Nature 440:918-921 [doi:10.1038/nature04617].

Reeburgh, W. S. 1980. Anaerobic methane oxidation: Rate depth distributions in Skan Bay sediments. Earth Planet. Sci. Lett. 47:345-352 [doi:10.1016/0012-821X(80)90021-7].

———. 2007. Oceanic methane biogeochemistry. Chem. Rev. 107:486-513 [doi:10.1021/cr050362v].

———, B. B. Ward, S. C. Whalen, K. A. Sandbeck, K. A. Kilpatrick, and L. J. Kerhof. 1991. Black-sea methane geochemistry. Deep-Sea Res. A 38:S1189-S1210.

Rehder, G., R. S. Keir, E. Suess, and M. Rhein. 1999. Methane in the northern Atlantic controlled by microbial oxidation and atmospheric history. Geophys. Res. Lett. 26(5):587-590.

Rudd, J. W. M., R. D. Hamilton, and N. E. Campbell. 1974. Measurement of microbial oxidation of methane in lake water. Limnol. Oceanogr. 19:519-524.

Sansone, F. J., and C. S. Martens. 1978. Methane oxidation in Cape Lookout Bight, North Carolina. Limnol. Oceanogr. 23(2):349-355 [doi:10.4319/lo.1978.23.2.0349].

Schlitzer, R. 2010. Ocean data view, <hppt://odv.awi.de>.

Scranton, M. I., and P. G. Brewer. 1978. Consumption of dissolved methane in the deep ocean. Limnol. Oceanogr. 23(6):1207-1213 [doi:10.4319/lo.1978.23.6.1207].

Southon, J. R., and G. M. Santos. 2004. Ion source development at KCCAMS, University of California, Irvine. Radiocarbon 46(1):33-39.

———, and ———. 2007. Life with MC-SNICS. Part II: further ion source development at the Keck carbon cycle AMS facility. Nucl. Instrum. Methods Phys. Res., Sect. B. 259:88-93.

Stuiver, M., and H. A. Polach. 1977. Discussion: Reporting 14C data. Radiocarbon 19:355-363.

Treude, T., A. Boetius, K. Knittell, K. Wallmann, and B. B. Jørgensen. 2003. Anaerobic oxidation of methane above gas hydrates at Hydrate Ridge, NE Pacific Ocean. Mar. Ecol. Prog. Ser. 264:1-14 [doi:10.3354/meps264001].

Turteltaub, K. W., and S. V. Vogel. 2000. Bioanalytical applications of accelerator mass spectrometry for pharmaceutical research. Curr. Pharm. Des. 6:991-1007 [doi:10.2174/1381612003400047].

Valentine, D. L., D. C. Blanton, W. S. Reeburgh, and M. Kastner. 2001. Water column methane oxidation adjacent to an area of active hydrate dissociation, Eel River Basin. Geochim. Cosmochim. Acta 65(16):2633-2640 [doi:10.1016/S0016-7037(01)00625-1].

———, and others. 2010. Propane respiration jump-starts microbial response to a deep oil spill. Science 330(6001):208-211 [doi:10.1126/science.1196830].

Ward, B. B. 1992. The subsurface methane maximum in the Southern California Bight. Continent. Shelf Res. 12(5/6):735-752 [doi:10.1016/0278-4343(92)90028-I].

———, Kilpatrick, K.A., Wopat, A.E., Minnich, E.C., and M. E. Lidstrom. 1989. Methane oxidation in Saanich Inlet during summer stratification. Continent. Shelf Res. 9(1):65-75. [doi:10.1016/0278-4343(89)90083-6].

———, ———, P. C. Novelli, and M. I. Scranton. 1987. Methane oxidation and methane fluxes in the ocean surface-layer and deep anoxic waters. Nature 327(6119):226-229 [doi:10.1038/327226a0].

———, and K. A. Kilpatrick. 1990. Relationship between substrate concentration and oxidation of ammonium and methane in a stratified water column. Continent. Shelf Res. 10(12):1193-1208 [doi:10.1016/0278-4343(90)90016-F].

Xu, X. M., S. E. Trumbore, S. H. Zheng, J. R. Southon, K. E. McDuffee, M. Luttgen, and J. C. Liu. 2007. Modifying a sealed tube zinc reduction method for preparation of AMS graphite targets: Reducing background and attaining high precision. Nucl. Instrum. Methods Phys. Res., Sect. B 259(1):320-329.